

NASA TECHNICAL
MEMORANDUM

NASA TM X-53506

August 29, 1966

NASA TM X-53506

ON DYNAMIC RESPONSE OF A RECTANGULAR PLATE
TO A SERIES OF MOVING LOADS

by FRANK C. LIU
Aero-Astroynamics Laboratory

NASA

FACILITY FORM 802

N67 14560	
(ACCESSION NUMBER)	(THRU)
45	
(PAGES)	(CODE)
TMX-53506	32
(NASA CR OR TMX OR AD NUMBER)	(CATEGORY)

*George C. Marshall
Space Flight Center,
Huntsville, Alabama*

GPO PRICE \$ _____

CFSTI PRICE(S) \$ _____

Hard copy (HC) 2.00

Microfiche (MF) .50

TECHNICAL MEMORANDUM X- 53506

ON DYNAMIC RESPONSE OF A RECTANGULAR PLATE TO A SERIES OF MOVING LOADS

By

Frank C. Liu

George C. Marshall Space Flight Center
Huntsville, Alabama

ABSTRACT

This report examines the effect of a series of evenly spaced moving loads on an elastic rectangular plate that is clamped at all edges. Two types of loads are treated: (1) a uniformly distributed pressure over a fractional length of the plate and (2) an impulsive load. All loads across a plate are considered uniform.

The solution of the partial differential equation of vibration of a plate is assumed in the form of a double series with the generalized coordinates solved by using the Laplace transform method. Viscous damping is included.

Based on a two-term approximation, the steady-state dynamic response of the plate is obtained in analytical form from which the upper bounds of the maximum deflection and maximum bending stress are formulated. Numerical examples are given to illustrate the effect of the thickness of the plate, the aspect ratio, and the velocity of loads on the dynamic response. Three types of resonance conditions are derived.

NASA-GEORGE C. MARSHALL SPACE FLIGHT CENTER

NASA-GEORGE C. MARSHALL SPACE FLIGHT CENTER

TECHNICAL MEMORANDUM X-53506

ON DYNAMIC RESPONSE OF A RECTANGULAR PLATE
TO A SERIES OF MOVING LOADS

By

Frank C. Liu

AERO-ASTRODYNAMICS LABORATORY
RESEARCH AND DEVELOPMENT OPERATIONS

TABLE OF CONTENTS

	Page
SUMMARY	1
INTRODUCTION	1
EQUATION OF MOTION	3
METHOD OF SOLUTION	4
Solution for Impulse Loads	8
Solution for Distributed Loads	16
RESONANCE OF PLATE	22
EXAMPLES AND DISCUSSION OF RESULTS	25
REFERENCES	31
APPENDIX A - FORMULATION OF $a_n(s)$	32
APPENDIX B - FORMULATION OF $f(t)$ AND $g(t)$	33
APPENDIX C - FORMULATION OF EQUATION (40)	36

LIST OF ILLUSTRATIONS

Figure	Title	Page
1.	Coordinates of Plate	2
2.	Nondimensional Frequencies	7
3.	Φ and x_w^* versus β	11
4.	S and x_σ^* versus β	13
5.	Time History of $r(t)$ and $q(t)$	17
6.	c^* and τ^* versus r	23
7.	Curves of $\frac{1}{2} c \lambda_n \tau = k\pi$	24
8.	A_1 and β versus r of Case I, Example 1.	26
9.	w^* versus r of Example 1	27
10.	σ^* versus r of Example 1	27
11.	A_1 versus r of Case II, Example 1	28
12.	β^* versus r of Case II, Example 1	28
13.	w^* and σ^* versus r for $\mu \ll 1$	29

LIST OF TABLES

Table	Title	Page
I.	Approximations for Three Special Cases	14

DEFINITION OF SYMBOLS

Symbol	Definition
a	Length of plate
$a_n (s)$	Coefficient of expansion, equation (8)
$A_{nm} (s)$	Generalized coordinates, equation (6)
b	Width of plate
b_m	Coefficient of expansion, equation (8)
\bar{c}	Velocity of loads
c_s	Nondimensional velocity of sound
$C(s)$	Equation (5)
D	$\frac{Eh^3}{12(1-\nu^2)}$, bending stiffness of plate
E	Modulus of elasticity
h	Thickness of plate
k_{in}	Coefficient of expansion, equation (11)
\bar{L}	Length of distributed loads
$L \{ \}, L^{-1} \{ \}$	Laplace transform operators
\bar{P}_0	Intensity of load
$p(x, y, t)$	Dynamic load function
r	a/b , plate aspect ratio
s	Laplace transform variable of \bar{t}
\bar{t}	Time variable

DEFINITION OF SYMBOLS (Concluded)

Symbol	Definition
$u(t)$	Unit step function
$w(\bar{x}, \bar{y}, \bar{t})$	Dynamic deflection of plate
\bar{x}, \bar{y}	Coordinates of plate
α_i	Constant of beam function ($\alpha_1 = .9825, \alpha_2 = 1.0008$)
β	$= A_2 / A_1$, amplitude ratio
δ_n	$= \lambda_n / \lambda_1$
$\delta(t)$	Dirac function
ζ	Damping factor
Θ_n	$= c \lambda_n$
λ_n	Eigenvalues of a clamped-clamped beam ($\lambda_1 = 4.7300 = 1.5056\pi$ $\lambda_2 = 7.8532 = 2.4997\pi$)
μ_n	$= \Theta_n / \omega_n$
ν	Poisson's ratio
ρ	Mass density of plate
σ	Bending stress
$\bar{\tau}$	Time interval between two consecutive loads
$\phi_n(z)$	Eigenfunction of a clamped-clamped beam
$\bar{\omega}_n$	$= \omega_n / T$, natural frequencies of plate
T	$= \frac{a^2}{\lambda_1^2} \sqrt{\frac{\rho h}{D}}$

Note: Barred symbols denote dimensional quantity, and unbarred symbols denote nondimensional quantity.

ON DYNAMIC RESPONSE OF A RECTANGULAR PLATE TO A SERIES OF MOVING LOADS

SUMMARY

This report examines the effect of a series of evenly-spaced moving loads on an elastic rectangular plate that is clamped at all edges. Two types of loads are treated: (1) a uniformly distributed pressure over a fractional length of the plate and (2) an impulsive load. All loads across a plate are considered uniform.

The solution of the partial differential equation of vibration of a plate is assumed in the form of a double series with the generalized coordinates solved by using the Laplace transform method. Viscous damping is included.

Based on a two-term approximation, the steady-state dynamic response of the plate is obtained in analytical form from which the upper bounds of the maximum deflection and maximum bending stress are formulated. Numerical examples are given to illustrate the effect of the thickness of the plate, the aspect ratio, and the velocity of loads on the dynamic response. Three types of resonance conditions are derived.

INTRODUCTION

The primary objective of this report is to determine the dynamic response of an elastic rectangular plate subjected to a series of evenly-spaced moving loads. Both a uniformly distributed pressure over a fractional length of plate and an impulsive load are treated herein. In fact, an impulsive load is a limiting case of a uniformly distributed pressure, when the length of the distributed pressure becomes infinitesimal while the product of length and intensity takes the finite value, P_0 .

There are some practical applications of the preceding mathematical model to acoustic problems or stress analysis of a shell structure in an aerodynamic flow. Consider a plate that is an idealized panel of an airplane wing, or a skin panel of a large shell structure, while the moving loads resemble

shock waves or pressure disturbance originating from a noise source. If the loads travel at very high speeds relative to the plate at sonic velocity for instance it takes less than one hundredth of a second for the load to go across a plate. When this is in the same order of magnitude as the period of vibration, resonance may take place under certain relationships between velocity of the loads and the natural frequency of the plate. Furthermore, conditions of resonance may be related to both velocity and frequency of the moving loads. A determination of the dynamic response of the plate at resonance conditions can also be made if the viscous damping factor is known. To a structural designer, all this information may be helpful for the determination of the optimum aspect ratio and thickness of the panel.

The assumption is made that the loads travel in one direction only and that the space between two consecutive loads is greater than the length of plate. Otherwise, the principle of superposition may apply. The coordinates and dimensions of the plate and loads are shown in Figure 1. Analysis begins with the vibration of a rectangular plate with clamped edges.

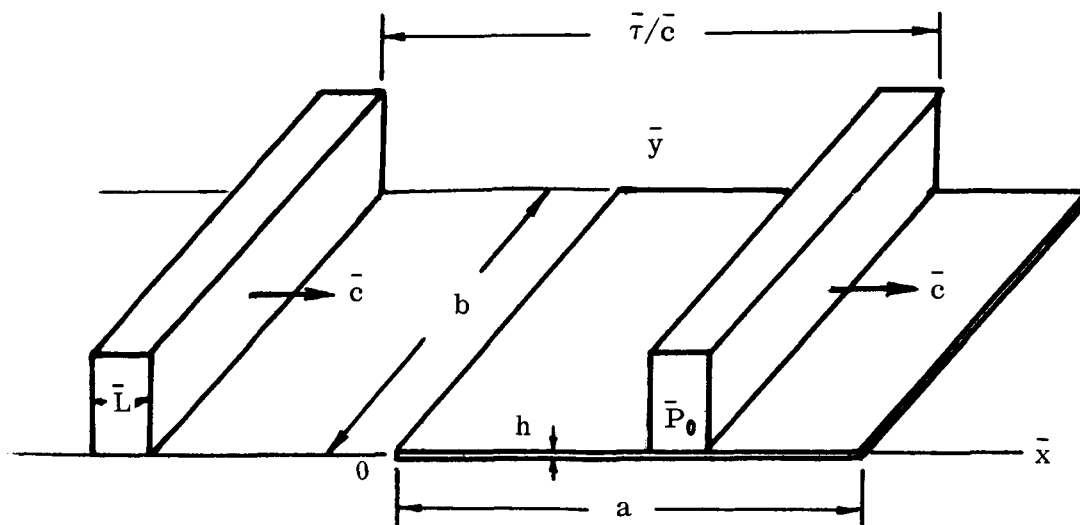


FIGURE 1. COORDINATES OF PLATE

EQUATION OF MOTION

The response of an elastic plate, $\bar{w}(\bar{x}, \bar{y}, \bar{t})$, to a dynamic load, $\bar{p}(\bar{x}, \bar{y}, \bar{t})$, is governed by the equation of vibration of a plate

$$D(\bar{w}_{xxxx} + 2\bar{w}_{xxyy} + \bar{w}_{yyyy}) + \rho h \bar{w}_{tt} = \bar{p}(\bar{x}, \bar{y}, \bar{t}) \quad (1)$$

with boundary conditions $\bar{w} = \frac{\partial \bar{w}}{\partial \bar{n}} = 0$ for clamped edges. The subscripts \bar{x}, \bar{y} , and \bar{t} denote the partial derivatives of \bar{w} . A symbol with a bar represents a dimensional quantity; the unbarred symbols denote the nondimensional quantity.

The function $\bar{p}(\bar{x}, \bar{y}, \bar{t})$ of the two types of moving loads to be treated can be expressed

For impulse loads ($\bar{L} \rightarrow 0$)

$$\bar{p}(\bar{x}, \bar{y}, \bar{t}) = \bar{P}_0 \sum_{k=0}^{\infty} \delta(\bar{t} - \bar{x}/\bar{c} - k\bar{\tau}), \quad (2a)$$

For distributed loads with length \bar{L} ($\bar{L} < a$)

$$\bar{p}(\bar{x}, \bar{y}, \bar{t}) = \bar{P}_0 \sum_{k=0}^{\infty} [u(\bar{t} - \bar{x}/\bar{c} - k\bar{\tau}) - u(\bar{t} - \frac{\bar{x} - \bar{L}}{\bar{c}} - k\bar{\tau})] \quad (2b)$$

where $\delta(\bar{t})$ is the Dirac function and $u(\bar{t})$ is the unit step function.

For convenience of manipulation, rewrite equation (1) in the nondimensional form

$$\frac{1}{\lambda_1^4} (w_{xxxx} + 2r^2 w_{xxyy} + r^4 w_{yyyy}) + w_{tt} = p(x, y, t) \quad (3)$$

The barred and unbarred symbols are related as follows

$$w = \bar{w}/a, \quad x = \bar{x}/a, \quad y = \bar{y}/a, \quad r = a/b, \quad L = \bar{L}/a$$

$$T = \sqrt{4\rho h/D\lambda_1^4}, \quad t = \bar{t}/T, \quad c = \bar{c}/a, \quad \tau = \bar{\tau}/T, \quad P_0 = \bar{P}_0 T^2 / \rho h = \frac{12(1-\nu^2) P_0 a^3}{\lambda_1^4 E h^3}$$

The definition of λ_1 is investigated in the succeeding section.

METHOD OF SOLUTION

Observing that $p(x, y, t)$ has a simple expression in Laplace transform, as a first step toward the solution of equation (3), we apply Laplace transformation to the partial differential equation with respect to the time variable. It follows immediately that

$$\frac{1}{\lambda_1^4} (W_{xxxx} + 2r^2 W_{xyyy} + r^4 W_{yyyy}) + s^2 W = P_0 C(s) e^{-sx/c} \quad (4)$$

where

$$W = W(x, y, s) = L\{w(x, y, t)\}$$

$$C(s) = \begin{cases} 1/(1 - e^{-\tau s}) & \text{for impulse loads} \\ (1 - e^{-sL/c})/s(1 - e^{-\tau s}) & \text{for distributed loads} \end{cases} \quad (5)$$

Note that the initial conditions $w(x, y, 0^+) = w_t(x, y, 0^+) = 0$ have been taken.

A well-known approach to the solution of equation (4) is to assume the solution in the form [2]

$$W(x, y, s) = \sum_{n=1}^{\infty} \sum_{m=1}^{\infty} A_{nm}(s) \phi_n(x) \phi_m(y) \quad (6)$$

The term $\phi_1(z)$ is the eigenfunction of the differential equation of a clamped-clamped beam,

$$\frac{d^4 \phi}{dz^4} - \lambda^4 \phi = 0,$$

with the boundary conditions $\phi(0) = \phi(1) = \phi'(0) = \phi'(1) = 0$. This assumed solution satisfies the boundary conditions along all four edges but does not satisfy the differential equation. However, the differential equation can be satisfied approximately by using the generalized Fourier series expansion. The sequence

$$\begin{aligned} \phi_i(z) &= \cosh \lambda_i z - \cos \lambda_i z - \alpha_i (\sinh \lambda_i z - \sin \lambda_i z) \quad i = 1, 2, \dots \quad (7) \\ \alpha_i &= (\cosh \lambda_i - \cos \lambda_i) / (\sinh \lambda_i - \sin \lambda_i) \end{aligned}$$

forms an orthogonal, complete set in the interval 0 to 1. This permits expansion of the term on the right-hand side of equation (4) in terms of $\phi_n(x)\phi_m(y)$

$$e^{-sx/c} = \sum_{m, n=1}^{\infty} a_n(s) b_m \phi_n(x) \phi_m(y) \quad (8)$$

where, as shown in Appendix A,

$$a_n(s) = \frac{c}{s^2 + \Theta_n^2} \left[\frac{2\Theta_n^2}{s + \Theta_n} - (-1)^n (s + \Theta_n) e^{-s/c} \right], \Theta_n = c\lambda_n$$

$$b_m = \begin{cases} 4\alpha_m / \lambda_m & m \text{ odd} \\ 0 & m \text{ even} \end{cases}$$

To take into account the damping effect on the vibration, assume that the damping is viscous and has a viscous damping coefficient of

$$e_{nm} \phi_n(x) \phi_m(y).$$

Substituting from equations (6) and (8) into equation (4) and adding the damping term leads to

$$\sum_{n, m=1}^{\infty} A_{nm} (\delta_n^4 + r^4 \delta_m^4 + e_{nm} s + s^2) \phi_n(x) \phi_m(y) + 2r^2 \delta_n^2 \delta_m^2 \phi_n''(x) \phi_m''(y)$$

$$= P_0 C(s) \sum_{n, m=1}^{\infty} a_n(s) b_m \phi_n(x) \phi_m(y) \quad (9)$$

where

$$\phi_i''(z) = \frac{1}{\lambda_i^2} \frac{d^2 \phi_i(z)}{dz^2} \quad \text{and} \quad \delta_i = \lambda_i / \lambda_1$$

It is now necessary to expand $\phi_j''(z)$ in terms of $\phi_i(z)$; this gives

$$\phi_j''(z) = \sum_{i=1}^{\infty} k_{ij} \phi_i(z) \quad (10)$$

The coefficients of expansion are [4]

$$k_{ij} = \int_0^1 \phi_j''(z) \phi_i(z) dz = 4 \left[1 + (-1)^{i+j} \right] \lambda_i^2 (\alpha_i \lambda_i - \alpha_j \lambda_j) / (\lambda_i^4 - \lambda_j^4) \quad i \neq j$$

$$k_{ii} = \int_0^1 \phi_i''(z) \phi_i(z) dz = (2 - \alpha_i \lambda_i) \alpha_i / \lambda_i \quad (11)$$

Substitution from equation (10) into equation (9) results in a set of an infinite number of simultaneous algebraic equations in the generalized coordinates $A_{nm}(s)$

$$(\delta_n^4 + r^4 \delta_m^4 + e_{nm} s + s^2) A_{nm} + \sum_{i,j=1}^{\infty} 2r^2 \delta_i^2 \delta_j^2 k_{ni} k_{mj} A_{ij} = P_0 a_n(s) b_m C(s). \quad (12)$$

$$n, m = 1, 2, \dots$$

Evidently, if a large number of equations is used to obtain the solution of equation (12), the expression of $A_{nm}(s)$ becomes cumbersome, and the task of finding inverse Laplace transforms becomes prohibitive. To serve the purpose of the present study, a simple approximation of $m = 1$ and $n = 1$ and 2 is made. The solution of $A_{11}(s)$ and $A_{21}(s)$ can then be readily obtained from the reduced system of equations

$$\begin{vmatrix} 1 + r^4 + 2r^2 k_{11}^2 + e_{11} s + s^2 & 0 \\ 0 & \delta_2^4 + r^4 + 2r^2 \delta_2^2 k_{22} k_{11} + e_{22} s + s^2 \end{vmatrix} \begin{vmatrix} A_{11} \\ A_{21} \end{vmatrix} = P_0 b_1 C(s) \begin{vmatrix} a_1(s) \\ a_2(s) \end{vmatrix} \quad (13)$$

Notice that equation (11) gives $k_{12} = k_{21} = 0$; consequently, the first two natural frequencies of the plate can be written out directly from equation (13).

$$\bar{\omega}_n = \omega_n / T = 2.267 \omega_n \left(\frac{\pi^2}{a^2} \sqrt{\frac{D}{\rho h}} \right)$$

$$\omega_n = \sqrt{\delta_n^4 + r^4 + 2 \delta_n^2 r^2 k_{11} k_{nn}} \quad (14)$$

The nondimensional frequencies versus the plate aspect ratio given by equation (14) are plotted in Figure 2.

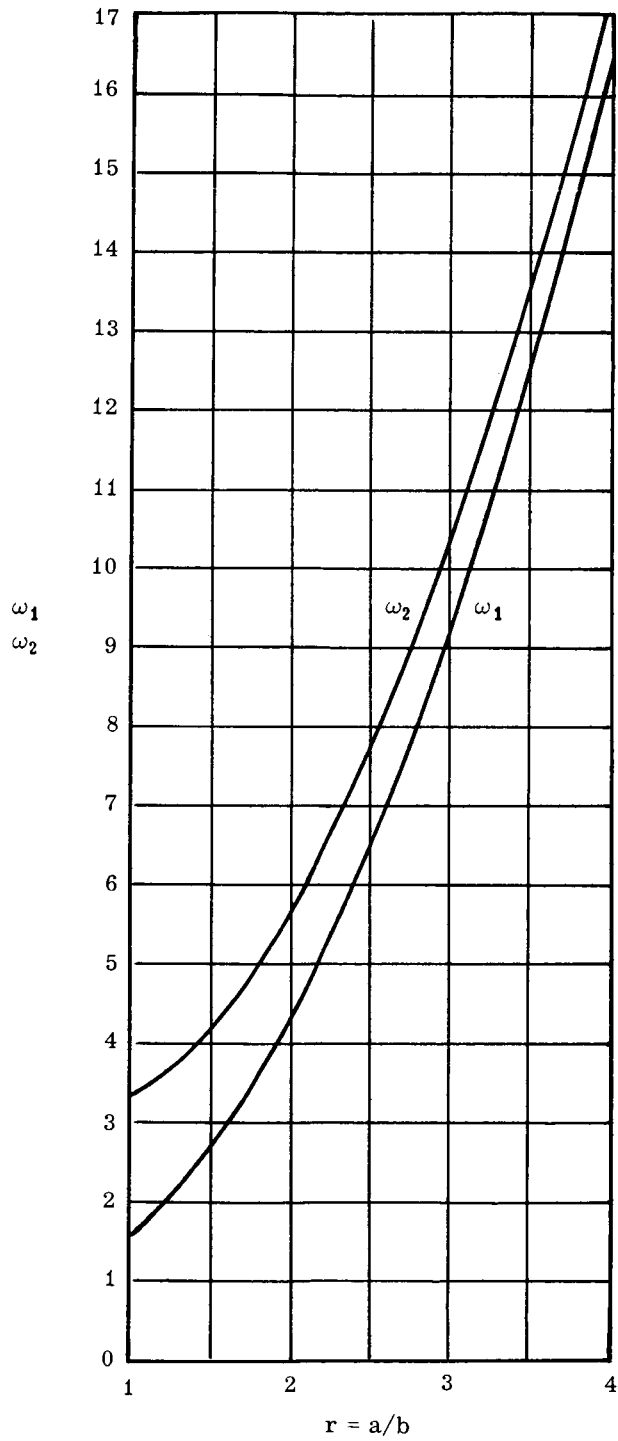


FIGURE 2. NONDIMENSIONAL FREQUENCIES

To further simplify the solution of A_{11} and A_{21} , assume that the damping factors for the first and second modes are equal.

$$\zeta = \frac{1}{2} e_{11} \omega_1 = \frac{1}{2} e_{22} \omega_2 \quad (15)$$

Hence, the damped natural frequencies of the plate become

$$\omega_{nd} = \omega_n \sqrt{1 - \zeta^2}$$

Express the solution of equation (13) in the form

$$A_{n1}(s) = P_0 b_1 (c/\omega_n^2) \left[R_n(s) + Q_n(s) e^{-s/c} \right] C(s), \quad (16)$$

where

$$R_n(s) = \frac{2\Theta_n^2}{(s+\Theta_n) \left[(s+\zeta\omega_n)^2 + \omega_{nd}^2 \right] (s^2 + \Theta_n^2)} \quad (17)$$

$$Q_n(s) = -(-1)^n \frac{(s+\Theta_n)}{\left[(s+\zeta\omega_n)^2 + \omega_{nd}^2 \right] (s^2 + \Theta_n^2)} \quad (18)$$

Determination of the inverse Laplace transform for the two types of loads will be given separately.

Solution for Impulse Loads

By using the method of partial fractions, $R_n(s)$ of equation (17) and $Q_n(s)$ of equation (18) can be written as a sum of five and four functions, respectively

$$R_n(s) = \sum_0^4 R_{nk} F_{nk}(s), \quad Q_n(s) = \sum_1^4 Q_{nk} F_{nk}(s). \quad (19)$$

The constants, R_{nk} , Q_{nk} , and the function, $F_{nk}(s)$, are shown in

Appendix B. For impulse loads, $C(s)$ of equation (16) is as noted in equation (5),

$$C(s) = \frac{1}{1 - e^{-\tau s}}.$$

It has been shown [5] that the inverse Laplace transform of a periodic function may be expressed in the form:

$$L^{-1} \left\{ \frac{F(s)}{1 - e^{-\tau s}} \right\} = \psi(\hat{t}) - \psi(t), \quad \begin{array}{l} K\tau < t < (K+1)\tau, \quad K = 1, 2, \dots \\ -\tau < \hat{t} < 0 \end{array} \quad (20)$$

in which $\psi(\hat{t})$ is a function of a discrete variable \hat{t} , and $\psi(t)$ is the same function of the continuous variable t . The Laplace transform pairs of F and ψ of equation (20) are given in Appendix B. As derived

$$\frac{1}{c} L^{-1} \left\{ \frac{R_n(s)}{1 - e^{-\tau s}} \right\} = R_{no} \left[\psi_{no}(\hat{t}) - \psi_{no}(t) \right] + f_{nr}(\hat{t}) - f_{nr}(t) + g_{nr}(\hat{t}) - g_{nr}(t) \quad (21a)$$

$$\frac{1}{c} L^{-1} \left\{ \frac{Q_n(s)}{1 - e^{-\tau s}} \right\} = f_{nq}(\hat{t}) - f_{nq}(t) + g_{nq}(\hat{t}) - g_{nq}(t) \quad (21b)$$

Finally, the inverse Laplace transform of equation (16) may be written in the form

$$L^{-1} \left\{ A_{n1}(s) \right\} = P_0 b_1 (c/\omega_n^2) \left[\hat{f}_n(\hat{t}) - f_n(t) + \hat{g}_n(\hat{t}) - g_n(t) \right], \quad (22)$$

where

$$f_n(t) = R_{no} \psi_{no}(t) + f_{nr}(t) - (-1)^n f_{nq}(t - \frac{1}{c}) u(t - \frac{1}{c}) \quad (22a)$$

$$g_n(t) = g_{nr}(t) - (-1)^n g_{nq}(t - \frac{1}{c}) u(t - \frac{1}{c}) \quad (22b)$$

$$\hat{f}_n(\hat{t}) = R_{no} \psi_{no}(\hat{t}) + f_{nr}(\hat{t}) - (-1)^n f_{nq}(\hat{t} + \iota\tau - \frac{1}{c}) \quad (22c)$$

$$\hat{g}_n(\hat{t}) = g_{nr}(\hat{t}) - (-1)^n g_{nq}(\hat{t} + \iota\tau - \frac{1}{c}) \quad (22d)$$

$$\text{when } -\tau < \hat{t} < -\tau + \frac{1}{c} \quad \iota = 1$$

$$\text{when } -\tau + \frac{1}{c} < t < 0 \quad \iota = 0; \text{ and } \hat{g}_n(\hat{t}) = g_n(\hat{t}), \hat{f}_n(\hat{t}) = f_n(\hat{t})$$

Substitution from equations (B-1c) and (B-1d) into equation (22b) yields

$$g_n(t) = \frac{1}{2} \sqrt{2B_n [1 - (-1)^n \sin \lambda_n]} \csc \frac{1}{2} \Theta_n \tau \sin[\Theta_n (t + \frac{1}{2}\tau) + \gamma_n + \eta_n] \text{ for } t > \frac{1}{c} \quad (22b')$$

For a steady-state solution, $f_n(t)$ and $g_n(t)$ can be disregarded because the former decreases exponentially with time while the coefficient of the latter is of a higher order of smallness ($\sin \lambda_n = (-1)^n$) except in the neighborhood of $\frac{1}{2} \Theta_n \tau = k\pi$.

As shown in Appendix B equations (22c) and (22d) can be rewritten as follows

$$\hat{f}(\hat{t}) = R_0 \psi_0(\hat{t}) + \hat{F} e^{-\zeta \omega \hat{t}} \cos(\omega \hat{t} - \phi - \psi) \quad (23a)$$

$$\hat{g}(\hat{t}) = \begin{cases} \sqrt{2B} \sin[\Theta(\hat{t} + \frac{1}{2}\tau) + \gamma + \hat{\eta}] & \text{when } -\tau < \hat{t} < -\tau + \frac{1}{c} \\ 0 & \text{when } -\tau + \frac{1}{c} < \hat{t} < 0, \text{ except in the neighborhood of} \\ \frac{1}{2} \Theta \tau = k\pi \end{cases} \quad (23b)$$

Hence, the two-term steady-state solution of the dynamic response of the plate is

$$w(x, y, t) = P_0 b_1 \sum_{n=1}^2 (c/\omega_n^2) [\hat{f}_n(\hat{t}) + \hat{g}_n(\hat{t})] \phi_n(x) \phi_1(y) \quad (24)$$

The Upper Bound of the Maximum Deflection and the Maximum Pending Stress. -

The maximum deflection and the maximum bending stress of the plate can be obtained by using equation (24), provided the greatest absolute value of $\hat{f}(\hat{t}) + \hat{g}(\hat{t})$ is determined. It is rather tedious to determine the greatest value of $\hat{f}(\hat{t}) + \hat{g}(\hat{t})$; however, the upper bound of this value, as denoted by $f^* + g^*$, can be written out immediately

$$f^* + g^* = \begin{cases} R_0 \psi_0(-\tau) + \hat{F} e^{\zeta \omega \tau} + \sqrt{2B} & -\tau < \hat{t} < -\tau + \frac{1}{c} \\ R_0 \psi_0(-\tau + \frac{1}{c}) + \hat{F} e^{\zeta \omega(\tau - \frac{1}{c})} & -\tau + \frac{1}{c} < \hat{t} < 0 \end{cases} \quad (25)$$

Hence, the upper bound of the maximum deflection may be expressed in the form

$$\bar{w}^* \leq a P_0 b_1 A_1 [\phi_1(x_W^*) + \beta \phi_2(x_W^*)] \phi_1(\frac{1}{2}) = w_0 A_1 \Phi \quad (26-1)$$

where

$$w_0 = aP_0 b_1 \phi_1 \left(\frac{1}{2}\right) = .02812 \frac{P_0 a^4}{Eh^3} \quad (\text{for } \nu = 1/3)$$

$$A_n = c (f_n^* + g_n^*) / \omega_n^2 \quad \beta = A_2/A_1 \quad (27)$$

$$\Phi = \phi_1(x_w^*) + \beta \phi_2(x_w^*) \quad (28)$$

The location of the maximum deflection which is denoted by x_w^* in the above equations can be determined numerically as a function of β from the equation

$$|\phi_1'(x)| + \delta_2 \beta |\phi_2'(x)| = 0 \quad (29)$$

where $\phi_n'(x) = \frac{1}{\lambda_n} \frac{d\phi_n}{dx}$. The graphs of x_w^* vs β and Φ vs β are shown in Figure 3.

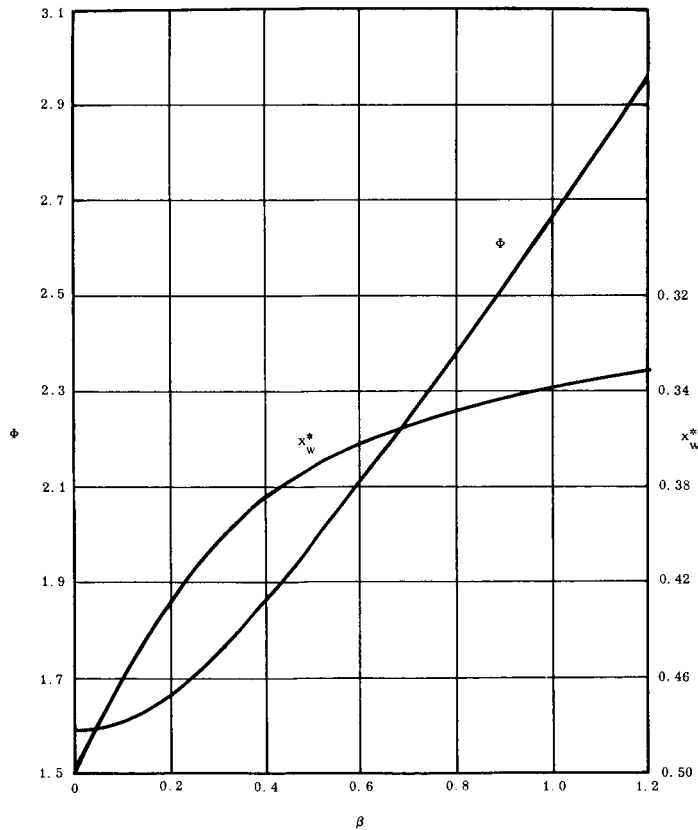


FIGURE 3. Φ and x_w^* VERSUS β

The upper bound of the maximum bending stress in x-direction can be determined by using the stress equation

$$\bar{\sigma}_x = \frac{Eh}{2(1-\nu)} \left[\frac{\partial^2 \bar{w}}{\partial x^2} + \nu \frac{\partial^2 \bar{w}}{\partial y^2} \right]$$

with $w(x, y, t)$ given by equation (24). Analogous to equation (26-1), express the upper bound of bending stress $\bar{\sigma}_x^*$ in the form

$$\bar{\sigma}_x^* \leq \sigma_0 A_1 \left[S_1(x_\sigma^*) + \beta S_2(x_\sigma^*) \right] \phi_1\left(\frac{1}{2}\right) = \sigma_0 A_1 S \quad (30-1)$$

where

$$\sigma_0 = P_0 b_1 \lambda_1^2 \phi_1\left(\frac{1}{2}\right) Eh / 2(1-\nu)a = 0.4718 \bar{P}_0 a^2 / h^2 \quad \left(\text{for } \nu = \frac{1}{3}\right)$$

$$S_n(x) = \left| \delta_n^2 \phi_n''(x) + \nu r^2 \phi_n(x) \phi_1'\left(\frac{1}{2}\right) / \phi_1\left(\frac{1}{2}\right) \right| \quad (31)$$

$$S = S_1(x_\sigma^*) + \beta S_2(x_\sigma^*) \quad (32)$$

The location of the maximum bending stress x_σ^* can be determined numerically as a function of β from the equation

$$\frac{dS_1(x)}{dx} + \beta \frac{dS_2(x)}{dx} = 0 \quad (33)$$

or

$$\phi_1'''(x) - 0.76545 \nu r^2 \phi_1'(x) + 4.5768\beta \left[\phi_2'''(x) - 0.2777 \nu r^2 \phi_2'(x) \right] = 0$$

where $\phi_n'''(x) = \frac{1}{\lambda_n^3} \frac{d^3 \phi_n}{dx^3}$. The graphs of x_σ^* vs β and S vs β are plotted in Figure 4.

To summarize, the procedure of computing the upper bound of the maximum deflection and the maximum bending stress is:

1. Determine ω_n from equation (14) or Figure 2

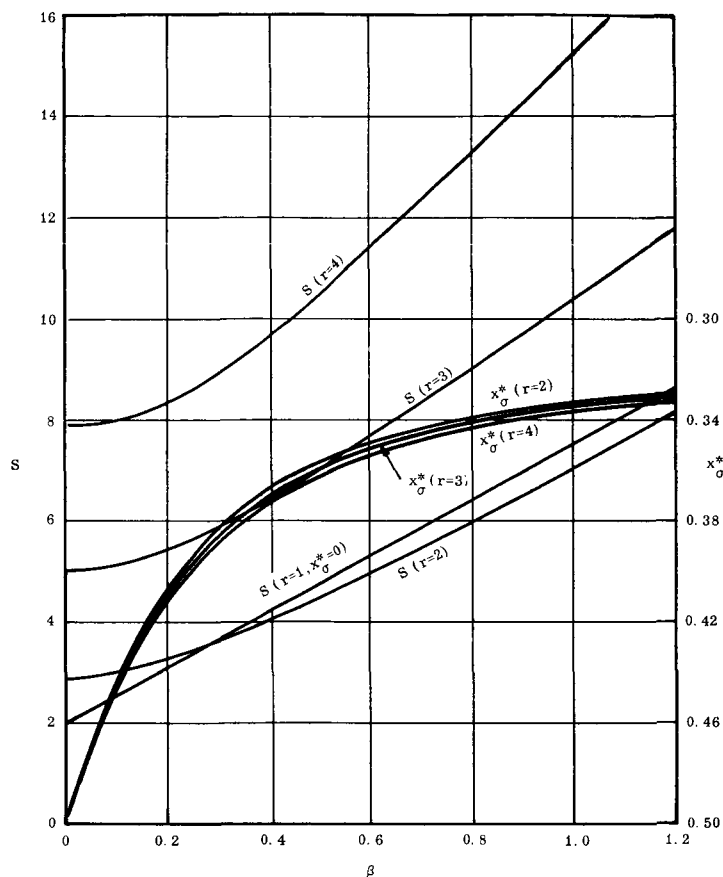


FIGURE 4. S AND x_σ^* VERSUS β

2. Compute f_n^* and g_n^* by using formulas in Appendix B and equation (25)
3. Obtain A_n and β from equation (27)
4. Read Φ and S from Figures 3 and 4, respectively
5. Calculate \bar{w}^* and $\bar{\sigma}_x^*$ from equations (26-1) and (30-1), respectively

Three Special Cases, $\mu_n \gg 1$, $\mu_n \ll 1$ and $\mu_n = 1$. - The three extreme cases, namely, $c \gg \omega_n / \lambda_n$, $c \ll \omega_n / \lambda_n$ and $c = \omega_n / \lambda_n$, deserve special attention.

Physically speaking, the first two conditions say that the frequencies of the velocity waves produced by the moving loads are very high and very low, respectively, in comparison with the natural frequency of the plate, and the third is a

condition of resonance at which the magnitude of the dynamic response has the greatest value. For these three cases, the constants given by the table in Appendix B and equations (21) and (B-2) have the approximate expressions given in Table I.

TABLE I. APPROXIMATIONS FOR THREE SPECIAL CASES

	$\mu_n \gg 1$	$\mu_n \ll 1$	$\mu_n = 1$
B	$1/\mu^4$	1	$1/4 \zeta^2$
C	$1/\mu^4$	1	$1/8 \zeta^2$
D	$-\mu^2$	1	2ζ
E	$-\mu^2$	1	-2ζ
F	μ^3	$3\zeta - \mu$	2ζ
G	μ^3	$\zeta - \mu$	2ζ
R ₀	$1/\mu^2$	1	$1/2(1-\zeta)$
R	$1/(\)\mu$	$\mu^2/(\)$	$\sqrt{2/4\zeta(1-\zeta)}(\)$
Q	$1/2(\)\mu$	$1/2(\)$	$\sqrt{2/8\zeta}(\)$
ξ	$\frac{1}{2}\pi$	$3\zeta - \mu$	$\frac{1}{4}\pi$
ϵ	$\frac{1}{2}\pi$	$\pi + \zeta - \mu$	$\frac{1}{4}\pi$
\hat{C}	$[2 - (-1)^n]Q$	$Qe^{-\zeta\omega(\alpha\tau - \frac{1}{c})}$	Q^*
\hat{D}	$2\sin^2 \frac{1}{2}\omega_d \tau$	1	\hat{D}

Note that in the above table () = $\cosh \zeta \omega \tau - \cos \omega_d \tau$ and

$$Q^* = Q \sqrt{\left(\frac{2}{1-\zeta}\right)^2 + e^{-2\zeta\omega(\tau - \frac{1}{c})} - (-1)^n \left(\frac{4}{1-\zeta}\right) e^{-\zeta\omega(\tau - \frac{1}{c})} \cos \omega_d(\tau - \frac{1}{c})}$$

Recall the original assumption that ζ is much smaller than one.

The values of ω_n/λ_n for plate aspect ratio $r = 1$ to 4 are as follows

	$r = 1$	$r = 2$	$r = 3$	$r = 4$
$n = 1$	0.341	0.933	1.975	3.450
$n = 2$	0.419	0.727	1.326	2.205

Case I $\mu_n \gg 1$ or $c \gg \omega_n/\lambda_n$

Since $\sqrt{2B + R_0}$ is negligible in comparison with $\hat{A} e^{\xi\omega\tau}$ in equation (25), reduce equation (27) to

$$A_n \cong \left[2 - (-1)^n \right] \frac{\sin^2 \frac{1}{2} \omega_d \tau}{\lambda_n \omega_n^2 (\cosh \xi \omega_n \tau - \cos \omega_{nd} \tau)} \quad (34)$$

This expression shows that the magnitude of the dynamic response is independent of the velocity of the moving loads when $c \gg \omega_n/\lambda_n$

Case II $\mu_n \ll 1$ or $c \ll \omega_n/\lambda_n$

Since $\tau > 1/c$ or τ is large, use the approximation

$$e^{\xi\omega\tau} / 2 (\cosh \xi\omega\tau - \cos \omega_d \tau) \cong 1$$

This results in

$$A_n \cong \left[1 + \sqrt{2} + e^{-\xi\omega(\tau - \frac{1}{c})} \right] c/\omega_n^2 \quad (35)$$

Thus, if the third term in the above equation is much smaller than one, the magnitude of the dynamic response is directly proportional to the velocity of the moving loads when $c \ll \omega_n/\lambda_n$.

Case III $\mu_n = 1$ or $c = \omega_n/\lambda_n$.

The magnitude of the dynamic response at resonance can be written in the form

$$A_n = \left[\frac{1}{2(1-\xi)} + \frac{\sqrt{2}}{2\xi} + D_n Q_n^* e^{\xi\omega_n \tau} \right] c/\omega_n^2 \quad (36)$$

At resonance, A_n is approximately inversely proportional to the damping factor ξ .

Solution for Distributed Loads

The inverse Laplace transform of equation (16) for the case of distributed loads becomes more cumbersome than for the impulse loads because of the complexity of $C(s)$ given by equation (5). It will simplify the problem somewhat if the damping factor is assumed equal to zero. Now, rewrite equation (16) in the form

$$A_{n1}(s) = \frac{P_0 b_1}{\lambda_n \omega_n^2} \left[R_n(s) - (-1)^n Q_n(s) e^{-\frac{s}{c}} \right] \left(\frac{1 - e^{-sL/c}}{1 - e^{-\tau s}} \right) \quad (37)$$

where

$$\begin{aligned} \lambda R(s) &= \frac{2\Theta^3 \omega^2}{s(s^2 + \omega^2)(s^2 + \Theta^2)(s + \Theta)} \\ &= \frac{2}{s} + \frac{2\mu^3}{\omega^4(1 - \mu^4)} \left(\frac{\mu s + \omega}{s^2 + \omega^2} \right) - \frac{1}{1 - \mu^2} \left(\frac{s + \Theta}{s^2 + \Theta^2} \right) - \frac{1}{1 + \mu^2} \left(\frac{1}{s + \Theta} \right) \end{aligned} \quad (38a)$$

$$\begin{aligned} \lambda Q(s) &= \frac{\Theta \omega^2 (s + \Theta)}{s(s^2 + \omega^2)(s^2 + \Theta^2)} \\ &= \frac{1}{s} + \frac{\mu}{\omega^2(1 - \mu^2)} \left(\frac{\mu s - \omega}{s^2 + \omega^2} \right) - \frac{1}{1 - \mu^2} \left(\frac{s - \Theta}{s^2 + \Theta^2} \right) \end{aligned} \quad (38b)$$

It follows immediately that

$$r(t) = L^{-1}\{R(s)\} = 2 + R \sin \omega(t + \gamma) + R' \sin \Theta(t + \frac{1}{4}\pi) + R'' e^{-\Theta t} \quad (39a)$$

$$q(t) = L^{-1}\{Q(s)\} = 1 + Q \sin \omega(t - \gamma) + Q' \sin \Theta(t - \frac{1}{4}\pi) \quad (39b)$$

where

$$\begin{aligned} R &= \frac{2\mu^3 \sqrt{1 + \mu^2}}{\omega^4(1 - \mu^4)} & Q &= \frac{\mu \sqrt{1 + \mu^2}}{\omega^2(1 - \mu^2)} \\ -R' &= Q' = \sqrt{2}/(1 - \mu^2) & R'' &= -1/(1 + \mu^2) & \gamma &= \tan^{-1} \mu \end{aligned}$$

Knowing the inverse Laplace transform of $R_n(s)$ and $Q_n(s)$, the inverse Laplace transform function of equation (37) denoted by

$$A_n(t) = L^{-1}\{A_{n1}(s)\}$$

can be illustrated diagrammatically (Fig. 5). This function can be expressed

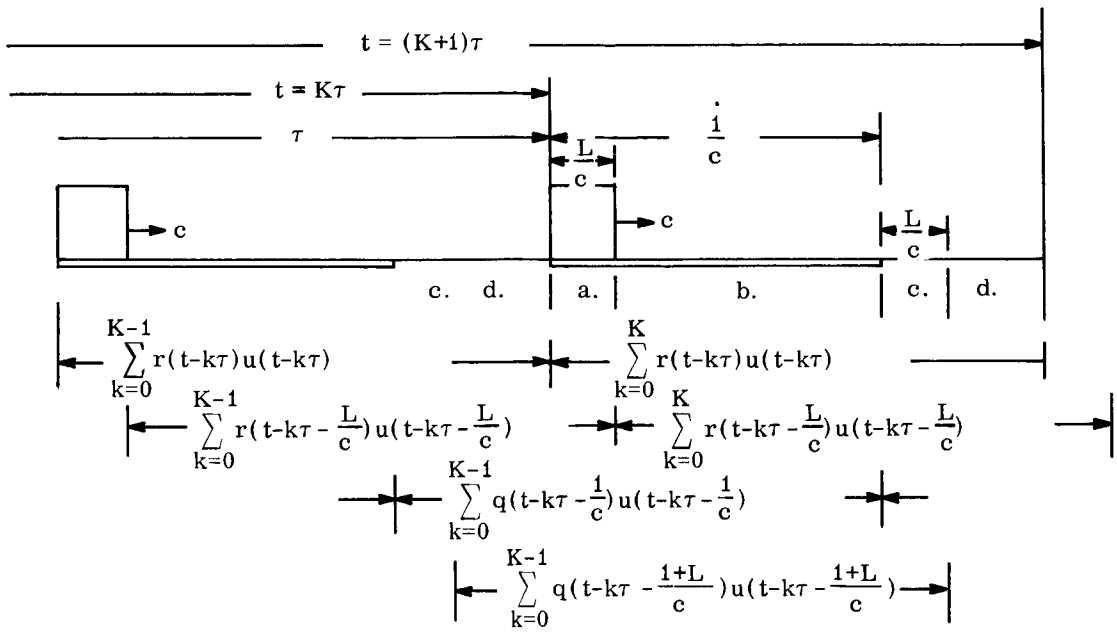


FIGURE 5. TIME HISTORY OF $r(t)$ AND $q(t)$

as sectional, continuous functions in four regions, a to d. With the aid of Figure 5 and the shorthand notation

$$f(K, \alpha) = \sum_{k=0}^{K} f(t-k\tau - \alpha) u(t - k\tau - \alpha)$$

write $A_n(t)$ as follows

Region a. $K\tau < t < K\tau + L/c$

$$A_n(t) = \frac{P_0 b_1}{\lambda_n \omega_n^2} \left\{ r_n(K, 0) - r_n\left(K-1, \frac{L}{c}\right) - (-1)^n \left[q_n\left(K-1, \frac{1}{c}\right) - q_n\left(K-1, \frac{1+L}{c}\right) \right] \right\} \quad (40)$$

Region b. $K\tau + \frac{L}{c} < t < K\tau + \frac{1}{c}$

$$A_n(t) = \frac{P_0 b_1}{\lambda_n \omega_n^2} \left\{ r_n\left(K, 0\right) - r_n\left(K, \frac{L}{c}\right) - (-1)^n \left[q_n\left(K-1, \frac{1}{c}\right) - q_n\left(K-1, \frac{1+L}{c}\right) \right] \right\} \quad (40b)$$

Region c. $K\tau + \frac{1}{c} < t < K\tau + \frac{1+L}{c}$

$$A_n(t) = \frac{P_0 b_1}{\lambda_n \omega_n^2} \left\{ r_n\left(K, 0\right) - r_n\left(K, \frac{L}{c}\right) - (-1)^n \left[q_n\left(K, \frac{1}{c}\right) - q_n\left(K-1, \frac{1+L}{c}\right) \right] \right\} \quad (40c)$$

Region d. $K\tau + \frac{1+L}{c} < t < (K+1)\tau$

$$A_n(t) = \frac{P_0 b_1}{\lambda_n \omega_n^2} \left\{ r_n\left(K, 0\right) - r_n\left(K, \frac{L}{c}\right) - (-1)^n \left[q_n\left(K, \frac{1}{c}\right) - q_n\left(K, \frac{1+L}{c}\right) \right] \right\} \quad (40d)$$

Making use of the formulas derived in Appendix C, combine the preceding four equations into a single equation of variable t_0 which is defined

$$t_0 = t - K\tau \text{ with } K = 1, 2, \dots \text{ and } K\tau < t < (K+1)\tau$$

$$\begin{aligned}
A(t) = & \frac{P_0 b_1}{\lambda \omega^2} \left\{ 2 \sin \frac{\omega L}{2c} \left[\csc \frac{1}{2} \omega \tau \left(R \sin \frac{1}{2} M \omega \tau \cos \left\{ \omega \left[t_0 + \left(K - \frac{M+1}{2} \right) \tau - \frac{L}{2c} \right] + \gamma \right\} \right. \right. \right. \\
& - (-1)^n Q \sin \frac{1}{2} P \omega \tau \cos \left\{ \omega \left[t_0 + \left(K - \frac{P+1}{2} \right) \tau - \frac{2+L}{2c} \right] - \gamma \right\} \left. \right. \\
& + R \cos \left[\omega \left(t_0 + K \tau - \frac{L}{2c} \right) + \gamma \right] \\
& - (-1)^n Q \cos \left[\omega \left(t_0 + K \tau - \frac{2+L}{2c} \right) - \gamma \right] \\
& + 2 \sin \frac{1}{2} \lambda L \left[\csc \frac{1}{2} c \lambda \tau R' \left(\sin \frac{1}{2} M c \lambda \tau \cos \left\{ c \lambda \left[t_0 + \left(K - \frac{M+1}{2} \right) \tau - \frac{L}{2c} \right] + \frac{1}{4} \pi \right\} \right. \right. \\
& - (-1)^n Q' \sin \frac{1}{2} P c \lambda \tau \cos \left\{ c \lambda \left[t_0 + \left(K - \frac{P+1}{2} \right) \tau - \frac{2+L}{2c} \right] - \frac{1}{4} \pi \right\} \left. \right. \\
& + R' \cos \left[c \lambda \left(t_0 + K \tau - \frac{L}{2c} \right) + \frac{1}{4} \pi \right] \\
& - (-1)^n Q' \cos \left[c \lambda \left(t_0 + K \tau - \frac{2+L}{2c} \right) - \frac{1}{4} \pi \right] \\
& + R'' e^{-c \lambda (t_0 + C \tau)} (1 - e^{\lambda L}) [1 - e^{-c \lambda (M+1) \tau}] (1 - e^{-c \lambda \tau})^{-1} \\
& + C [2 + R \sin (\omega t_0 + \gamma) + R' \sin (c \lambda t_0 + \frac{1}{4} \pi) + R'' e^{-c \lambda t_0}] \\
& \left. - (-1)^n D \left[1 + Q \sin \left[\omega \left(t_0 - \frac{1}{c} \right) - \gamma \right] + Q' \sin \left[c \lambda \left(t_0 - \frac{1}{c} \right) - \frac{1}{4} \pi \right] \right] \right\} \quad (41)
\end{aligned}$$

The values of the constants M, P, C, and D in the above equation are as follows:

	t_0	M	P	C	D
a	$0 \leq t_0 \leq L/c$	K-1	K-1	1	0
b	$L/c \leq t_0 \leq 1/c$	K	K-1	0	0
c	$1/c \leq t_0 \leq (L+1)/c$	K	K-1	0	1
d	$(L+1)/c \leq t_0 \leq \tau$	K	K	0	0

Note that for brevity all the subscripts "n" are omitted from the symbols A(t), R, R', R'' Q, Q', λ , γ and ω .

For the case $K < 1$, this problem can be treated as a plate subjected to a single moving load and is given in the next section.

Now, the dynamic response of the plate is

$$\bar{w}(x, y, t) = aP_0b_1 \sum_{n=1}^2 A_n(t) \phi_n(x) \phi_1(y) \quad (42)$$

And

$$B_n(x, y) = \bar{w}_{xx} + \nu \bar{w}_{yy} = \lambda_1^2 [\delta_n^2 \phi_n''(x) \phi_1(y) + \nu r^2 \phi_n(x) \phi_1''(y)] \quad (43)$$

Then, the dynamic bending stress in x-direction is

$$\bar{\sigma}_x(x, y, t) = \frac{P_0b_1Eh}{2(1-\nu)a} \sum_{n=1}^2 A_n(t) B_n(x, y) \quad (44)$$

Using the symbol A_n^* to represent the maximum absolute value of $A_n(t)$ and $\beta = A_2^*/A_1^*$, obtain the upper bound of the maximum deflection

$$\bar{w}^* = w_0 A_1^* \Phi \quad (26-2)$$

and the upper bound of the maximum bending stress

$$\bar{\sigma}^* = \sigma_0 A_1^* S \quad (30-2)$$

where the symbols w_0 , σ_0 , Φ and S are defined previously in equations (26-1) and (30-1).

It is difficult to tell at what time region A_n^* occurs. This suggests a procedure of computing the greatest value of $A_n(t)$ in each region and choosing the largest one among them. Let F_a to F_d denote the greatest value of $A_n(t)$ in regions a to d; hence

$$A_n^* = \text{Max}(F_a, F_b, F_c, F_d) \quad (45)$$

A simple but crude method of determining F is to let all the sines and cosines of equation (41) equal to one and add the absolute value of all terms. This can be refined by first combining the cosines of the same frequency and then summing the absolute values term by term.

A Single Moving Distributed Load - For a single moving distributed load, the load function given by equation (5) becomes

$$L \{p(x, y, t)\} = \frac{1}{s} e^{-sx/c} (1 - e^{-sL/c}) \quad (46)$$

Consequently

$$L^{-1} \{A_{n1}(s)\} = \frac{P_0 b_1}{\lambda_n \omega_n^2} \left\{ r_n(t) - r_n(t-L/c) u(t-L/c) \right. \\ \left. - (-1)^n \left[q_n(t-1/c) u(t-1/c) - q_n\left(t - \frac{1+L}{c}\right) u\left(t - \frac{1+L}{c}\right) \right] \right\} \quad (47)$$

Hence, equation (41) reduces to

$$A_n(t) = \frac{P_0 b_1}{\lambda_n \omega_n^2} \left\{ 2 \sin \omega_n L/2c \left(AR_n \cos [\omega_n(t-L/2c) + \gamma_n] \right. \right. \\ \left. \left. - (-1)^n BQ_n \cos \left[\omega_n \left(t - \frac{1+\frac{1}{2}L}{c} \right) - \gamma_n \right] \right) \right. \\ \left. + 2 \sin \frac{1}{2} \lambda_n L \left(AR'_n \cos [\Theta_n(t-L/2c) + \frac{1}{4}\pi] \right. \right. \\ \left. \left. - (-1)^n BQ'_n \cos \left[\Theta_n \left(t - \frac{1+\frac{1}{2}L}{c} \right) - \frac{1}{4}\pi \right] \right) \right. \\ \left. - AR''_n (e^{\lambda_n L} - 1) e^{-\Theta_n t} \right. \\ \left. + C \left[2 + R_n \sin(\omega_n t + \gamma_n) + R'_n \sin(\Theta_n + \frac{1}{4}\pi) + R''_n e^{-\Theta_n t} \right] \right. \\ \left. - (-1)^n D \left(1 + Q_n \sin[\omega_n(t-1/c) - \gamma_n] + Q'_n \sin[\Theta_n(t-1/c) - \frac{1}{4}\pi] \right) \right\} \quad (48)$$

where A, B, C and D have the following tabulated values

		A	B	C	D
$0 < t < \frac{L}{c}$	a	0	0	1	0
$\frac{L}{c} < t < \frac{1}{e}$	b	1	0	0	0
$\frac{1}{c} < t < \frac{1+L}{c}$	c	1	0	0	1
$\frac{1+L}{c} < t$	d	1	1	0	0

RESONANCE OF PLATE

There are three conditions which may cause resonance of the plate to take place.

1. Frequency resonance, $\frac{1}{2}\omega_n \tau = k\pi$

For the case of impulse load, the functions ψ_{n1} and ψ_{n2} become very large if the damping factor is very small and for distributed load $A_n(t)$, given by equation (41), become infinite. The critical values of τ , $\tau^* = 2\pi k/\omega_n$, versus the plate aspect ratio are plotted in Figure 6.

2. Velocity resonance, $\mu_n = 1$ or $c_n = \omega_n / \lambda_n$

When the frequency of the velocity waves produced by the traveling loads coincides with the natural frequency of the plate, the coefficients R_k and Q_k become very large for a small damping factor, as shown in Appendix B for the case of impulse loads. For distributed loads, it can be seen from equations (38a) and (38b) that the inverse Laplace transforms will have a term

$$L^{-1} \left[\frac{2s\omega}{(s^2 + \omega^2)^2} \right] = t \sin \omega t.$$

The critical values of c , $c^* = \omega_n / \lambda_n$, versus the plate aspect ratio are plotted also in Figure 6. The nondimensional velocity of sound at standard atmosphere is $c_s = \bar{c}_s \gamma / a \cong 0.01 (a/h)$ for both steel and aluminum plates.

3. Velocity-frequency resonance, $c\tau = 2k\pi / \lambda_n$

Under this condition both $g_n(t)$, given by equation (22b'), and $A_n(t)$ given by equation (41), become unbounded. The critical values of τ versus c are plotted in Figure 7. However, because of the smallness of the coefficient of $g_n(t)$, this condition should not impose serious response for the case of impulsive loads.

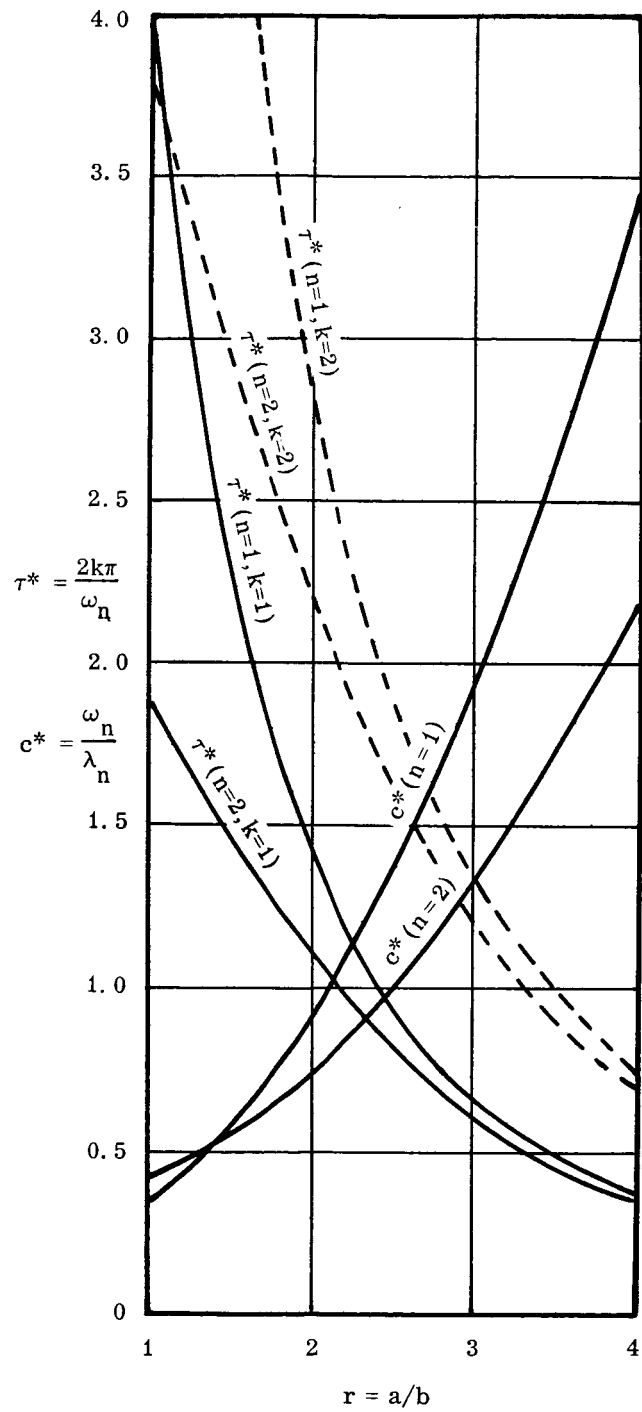


FIGURE 6. c^* AND τ^* VERSUS r

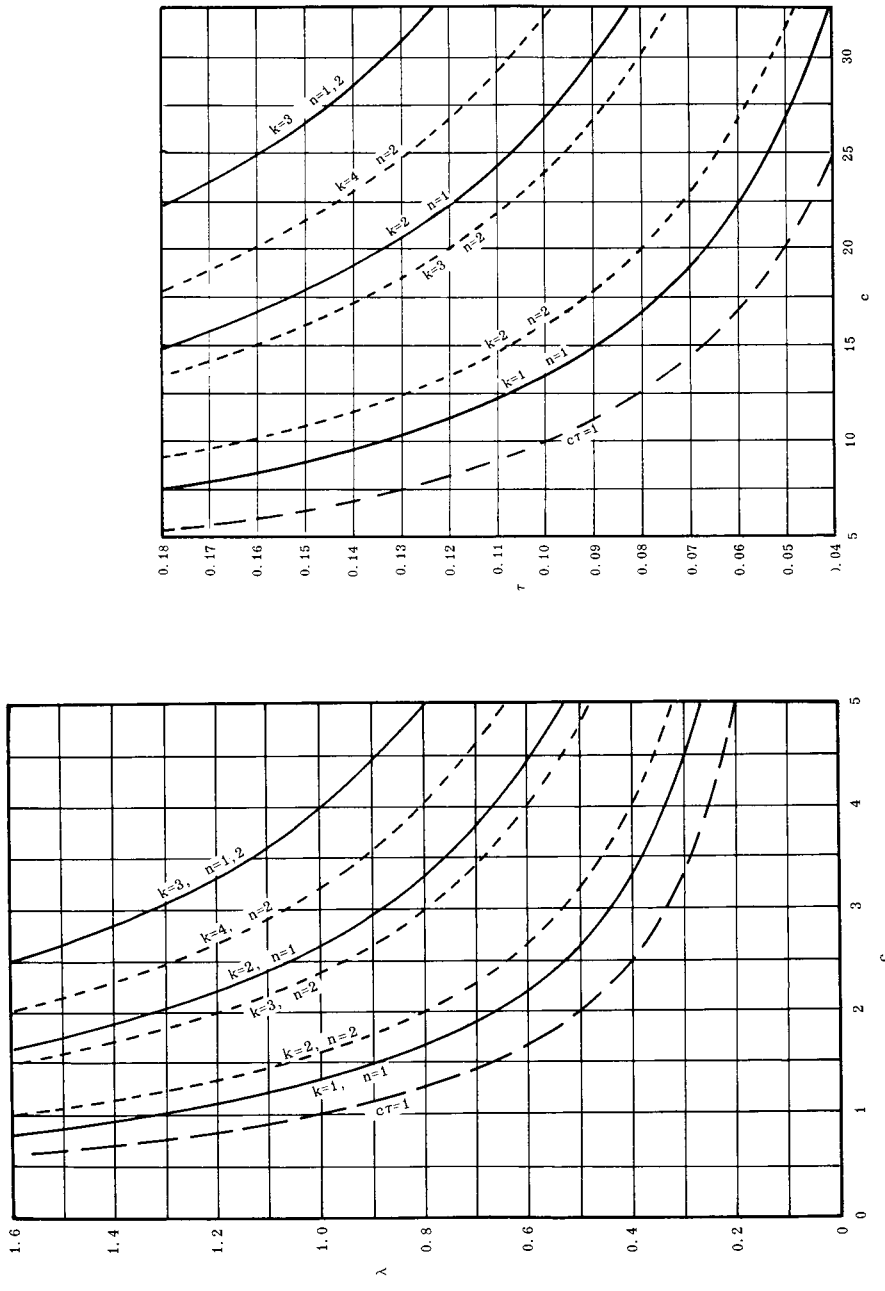


FIGURE 7. CURVES OF $\frac{1}{2}c\lambda, \tau = k\pi$

EXAMPLES AND DISCUSSION OF RESULTS

Examples on a plate subjected to a series of impulses:

Example 1. - Consider a steel plate with the following data

$$a = 0.6096\text{m (24 in.)}, \quad \zeta = 0.1, \quad \nu = 1/3$$

$$E = 20.67\text{N/m}^2 (30 \times 10^6 \text{ psi}), \quad \rho = 7855 \text{ Kg/m}^3 (15.24 \text{ slug/ft}^3)$$

Consider also that velocity of the moving impulses is in the neighborhood of the speed of sound in a standard atmosphere. Now, examine how the stiffness of the plate affects the dynamic response by taking $h = 0.0254 \text{ mm (0.01 in.)}$ and $h = 0.0803 \text{ mm (0.03162 in.)}$, respectively.

Case I. $h = 0.0254 \text{ mm (0.01 in.)}$

From the given data, calculate

$$T = \frac{a^2}{\lambda_1^2} \sqrt{\frac{\rho h}{D}} = 0.04186 \quad \tau = 1/\bar{f}T = 0.09 \quad c_s = \bar{c}_s T/a = 23.41$$

where c_s is the nondimensional velocity of sound. The values of $\mu_n = c\lambda_n/\omega_n$ of this velocity for plate aspect ratio $r = 1$ to 4 are as follows

	$r = 1$	$r = 2$	$r = 3$	$r = 4$
$n = 1$	68.7	25.1	11.84	6.78
$n = 2$	55.7	32.1	17.56	10.63

The values of A_1 and β are computed for the arbitrarily chosen velocities $c = 15, 20$ and 25 . The results show that there is no appreciable difference for the three velocities because c is much greater than ω_n/λ_n . Figure 8 shows A_1 and β versus r . Note that for these velocities the approximate expression given by equation (34) is applicable.

To calculate the upper bound of the maximum deflection and maximum bending stress, first read the value of A_1 and β from Figure 8 and Φ and S from Figures 3 and 4, respectively; then use equations (26-1) and (30-1). The results of w^* and σ^* versus the plate aspect ratio are plotted in Figures 9 and 10.

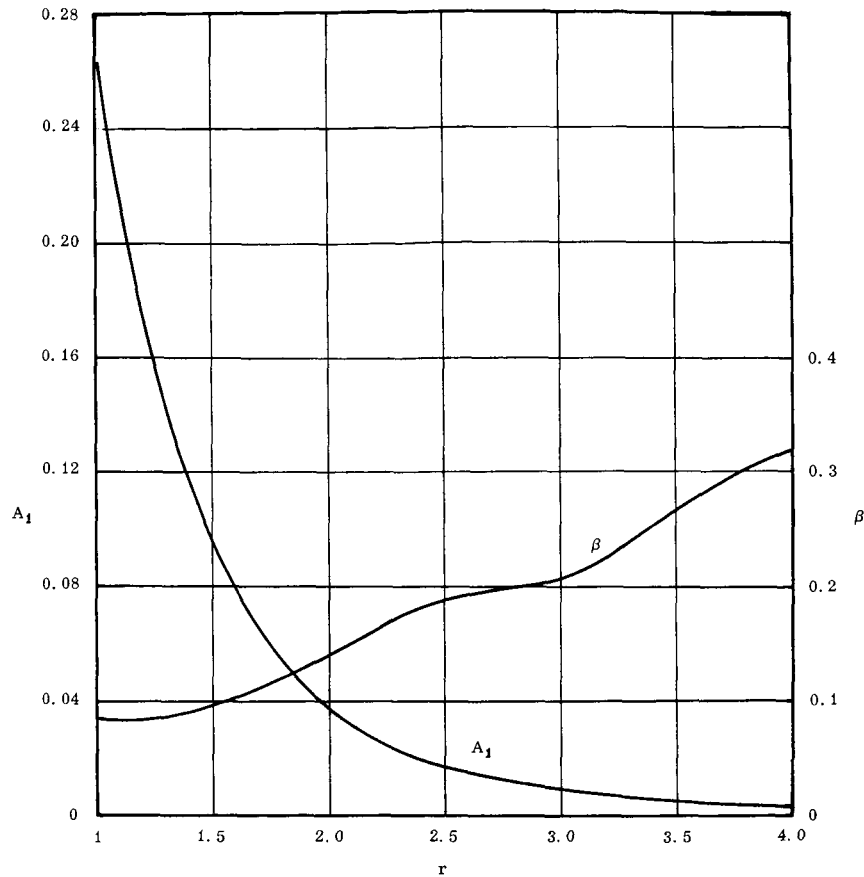


FIGURE 8. A_1 AND β VERSUS r OF CASE I, EXAMPLE 1

Case II $h = 0.0803$ mm (0.03162 in.). Increase the thickness of the plate by $\sqrt{10}$ times that of Case I, the values of T , c and μ_n are reduced to $1/10$ of the values calculated in Case I ($\tau = 0.9$). Plots of A_1 and β versus r for $c = 1.5, 2.0$ and 2.5 (c_s is 2.341 for this case) are shown in Figures 11 and 12 respectively. Figures 9 and 10 show the upper bound of the maximum deflection and maximum bending stress versus r .

Example 2. - Considering again a clamped plate subjected to a series of impulses, assume that the nondimensional velocity of the impulses are small so that $c \ll \omega_n / \lambda_n$ and $e^{-\zeta \omega (\tau - \frac{1}{c})} \ll 1$. By applying the approximation given by equation (35), obtain A_1 and β for various values of r . The upper bounds of the maximum deflection and maximum bending stress are shown in Figure 13.

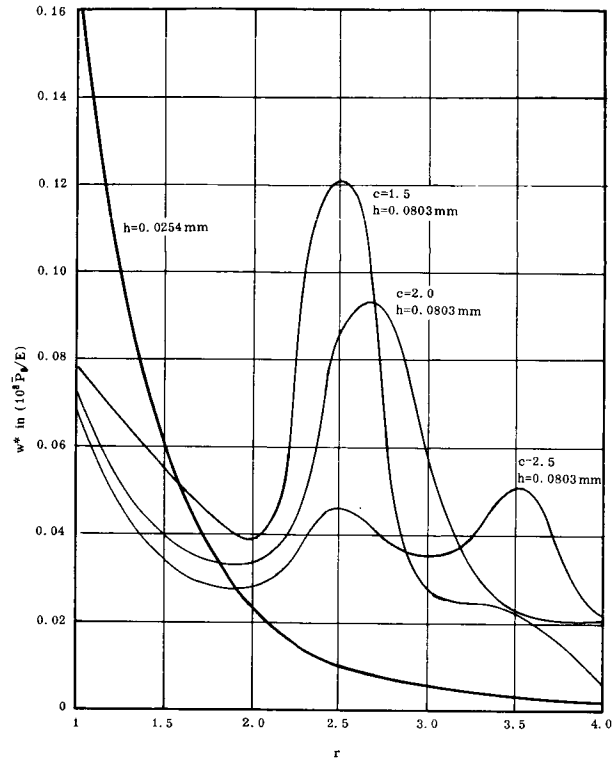


FIGURE 9. w^* VERSUS r OF EXAMPLE 1

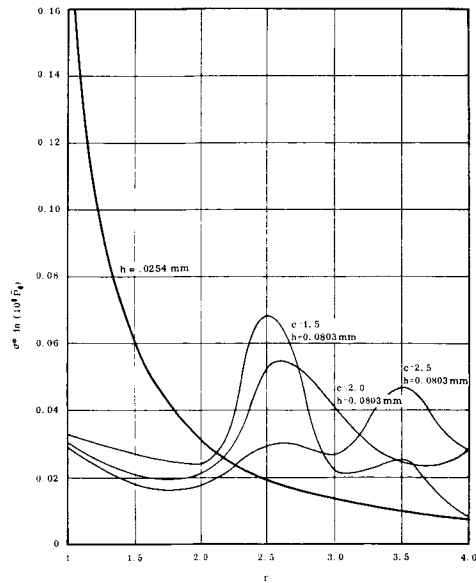


FIGURE 10. σ^* VERSUS r OF EXAMPLE 1

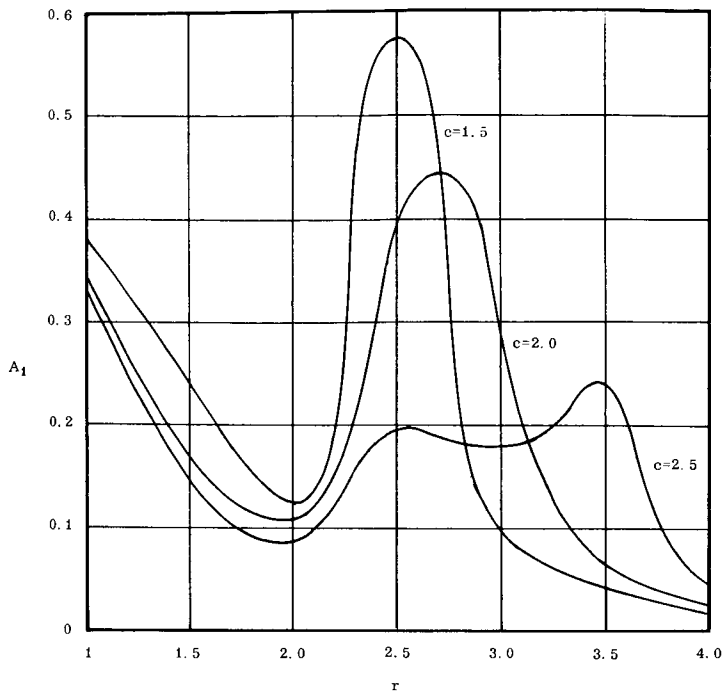


FIGURE 11. A_1 VERSUS r OF CASE II, EXAMPLE 1

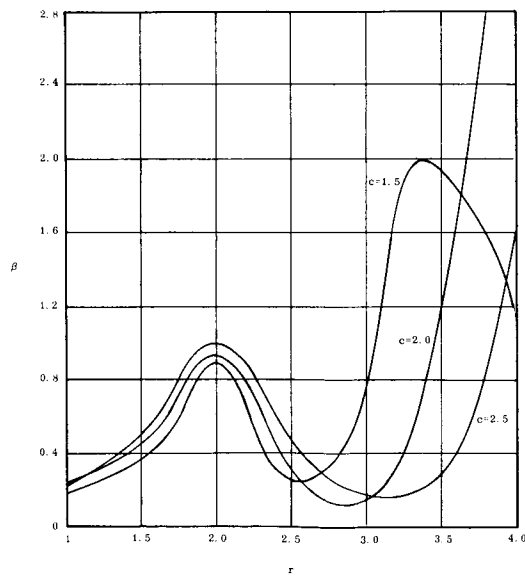


FIGURE 12. β^* VERSUS r OF CASE II, EXAMPLE 1

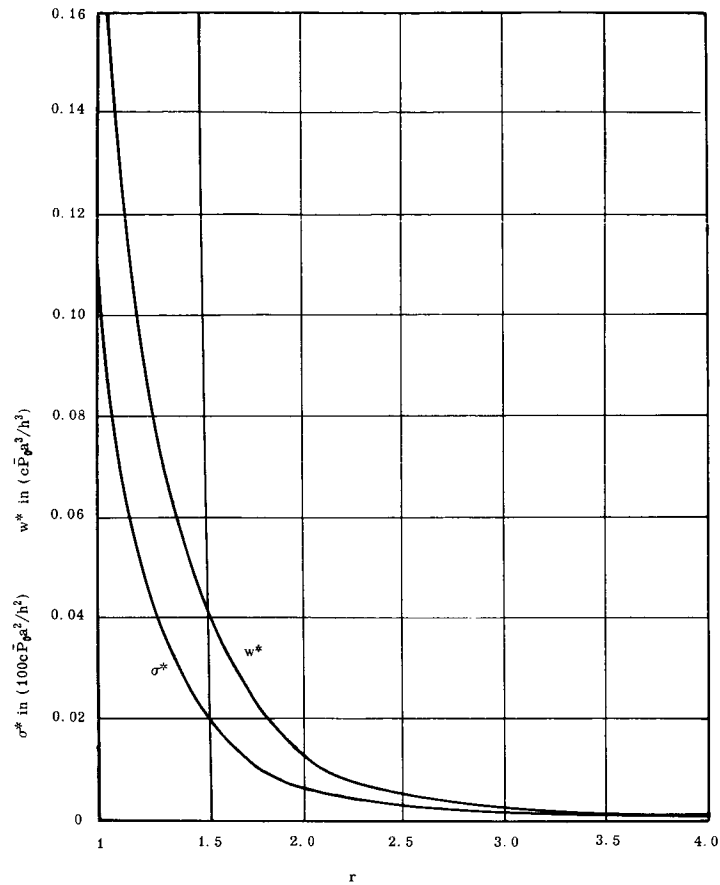


FIGURE 13. w^* AND σ^* VERSUS r FOR $\mu \ll 1$

Discussion of Results. - For a given frequency of the moving impulsive loads, the effects of the thickness of the plate, the plate aspect ratio, and the velocity of the loads on the dynamic responses are illustrated in Figures 8 to 13. Some interesting results have been observed:

1. If $c \gg \omega_n / \lambda_n$ (i. e., with high velocity loads moving on a thin plate), the dynamic response of the plate is almost independent of the velocity.
2. If $c \ll \omega_n / \lambda_n$, the dynamic response is directly proportional to the velocity.
3. The three conditions of resonance with either $n = 1$ or 2 are:

$$(1) \quad c = \omega_n / \lambda_n$$

$$(2) \tau = 2k\pi/\omega_n$$

$$(3) \frac{1}{2}c\lambda_n \tau = k\pi \quad (\text{this condition has no significant in reality})$$

For a plate with large damping, condition (1) is a predominant factor; while condition (2) is more important for small damping.

4. The peaks of the curves in Figure 11 correspond to the critical values of c and τ given by Figure 6.

5. The value of $\beta (= A_2/A_1)$ is small for a plate with panel aspect ratio close to one. This is an indication that the two-term approximation used in solving equation (13) is adequate (more terms are required to cope with the higher modes if r is large).

6. Since the w^* and σ^* presented here are the upper bounds of the dynamic response; in reality, these values could be considerably higher than the actual.

REFERENCES

1. Timoshenko, S.: *Vibration Problems in Engineering*. Third ed. D. Van Nostrand Co., 1955, pp. 351-356.
2. Nowacki, W. (Translation): *Dynamics of Elastic Systems*, John Wiley and Sons, Inc., 1963, pp. 240-243.
3. Young, D.; and Felgar, R. P.: *Tables of Characteristic Functions Representing Normal Modes of Vibration of a Beam*. University of Texas (Austin, Texas), July 1, 1949.
4. Felgar, R. P.: *Formulas for Integrals Containing Characteristic Functions of a Vibrating Beam*. University of Texas (Austin, Texas), Bureau of Engineering Research, 1950.
5. Wylie, C. R., Jr.: *Advanced Engineering Mathematics*. Second ed. McGraw-Hill Book Company, 1960, pp. 324-331.

APPENDIX A. FORMULATION OF $a_n(s)$

By definition of equation (8),

$$\begin{aligned}
 a(s) &= \int_0^1 e^{-sx/c} [\text{ch } \lambda x - \cos \lambda x - \alpha (\text{sh } \lambda x - \sin \lambda x)] dx \\
 &= \left\{ \frac{e^{-s/c}}{\text{sh } \lambda - \sin \lambda} \left[\left(-\frac{s}{c} \text{ch } \lambda - \lambda \text{sh } \lambda \right) (\text{sh } \lambda - \sin \lambda) + \left(\frac{s}{c} \text{sh } \lambda + \lambda \text{ch } \lambda \right) (\text{ch } \lambda - \cos \lambda) \right] \right. \\
 &\quad \left. + \left(\frac{s}{c} - \alpha \lambda \right) \right\} / (s^2/c^2 - \lambda^2) \\
 &\quad - \left\{ e^{-s/c} \left[\left(-\frac{s}{c} \cos \lambda + \lambda \sin \lambda \right) + \alpha \left(\frac{s}{c} \sin \lambda + \lambda \cos \lambda \right) \right] + \frac{s}{c} - \alpha \lambda \right\} / (s^2/c^2 + \lambda^2).
 \end{aligned}$$

Using the approximations

$$\alpha_n = 1, \quad \cos \lambda_n = 0, \quad \sin \lambda_n = (-1)^n, \quad \text{and } \text{ch } \lambda_n \cong \text{sh } \lambda_n,$$

obtain

$$a_n(s) \cong \frac{2c(c\lambda_n)^2}{(s + c\lambda_n)(s^2 + c^2\lambda_n^2)} - (-1)^n ce^{-s/c} \left(\frac{s + c\lambda_n}{s^2 + c^2\lambda_n^2} \right).$$

APPENDIX B. FORMULATION OF f(t) AND g(t)

The terms contained in equation (19) are tabulated as follows:

Laplace Transform Pairs and Coefficients of R(s) and Q(s)

k	$F_k(s)$	$\psi_k(z)$	R_k	Q_k
0	$\frac{1}{s + \Theta}$	$\frac{e^{-\Theta z}}{e^{\Theta \tau} - 1}$	$\frac{1}{1 + \mu^2 - 2\zeta\mu}$	0
1	$\frac{s + \zeta\omega}{(s + \zeta\omega)^2 + \omega_d^2}$	$\frac{e^{-\zeta\omega z} \cos\omega_d(z + \tau) - e^{-\zeta\omega(z + \tau)} \cos\omega_d \tau}{2(\cosh\zeta\omega\tau - \cos\omega_d\tau)}$	$2\mu^2 R_0 BD$	-CE
2	$\frac{\omega_d}{(s + \zeta\omega)^2 + \omega_d^2}$	$\frac{e^{-\zeta\omega z} \sin\omega_d(z + \tau) - e^{-\zeta\omega(z + \tau)} \sin\omega_d \tau}{2(\cosh\zeta\omega\tau - \cos\omega_d\tau)}$	$2\mu^2 R_0 BF$	CG
3	$\frac{s}{s^2 + \Theta^2}$	$-\frac{1}{2} \csc\frac{1}{2}\Theta\tau \sin\Theta(z + \frac{1}{2}\tau)$	-BD	BE
4	$\frac{\Theta}{s^2 + \Theta^2}$	$\frac{1}{2} \csc\frac{1}{2}\Theta\tau \cos\Theta(z + \frac{1}{2}\tau)$	BE	BD

Definition of Constants

$$B = [(1 - \mu^2)^2 + 4\zeta^2 \mu^2]^{-1}$$

$$C = [(1 - \mu^2)^2 + 8\zeta^2 \mu^2]^{-1}$$

$$D = 1 - \mu^2 + 2\zeta\mu$$

$$E = 1 - \mu^2 - 2\zeta\mu$$

$$F = \mu(\mu^2 - 1) - \zeta(\mu^2 - 3)$$

$$G = \mu(\mu^2 - 1) + \zeta(\mu^2 + 1)$$

Notice that the subscripts "n" are omitted from all the symbols except s, z, ζ , and τ , and that the constants B to G are approximations after neglecting the higher order terms of ζ .

Further simplification by combining ψ_1, ψ_2 and ψ_3, ψ_4 , respectively, results in

$$f_r(z) = R_1\psi_1(z) + R_2\psi_2(z) \quad (\text{B-1a})$$

$$= R \left\{ e^{-\zeta\omega z} \cos[\omega_d(z+\tau) - \xi] - e^{-\zeta\omega(z+\tau)} \cos(\omega_d z - \xi) \right\}$$

$$f_q(z) = Q_1\psi_1(z) + Q_2\psi_2(z) \quad (\text{B-1b})$$

$$= Q \left\{ e^{-\zeta\omega z} \cos[\omega_d(z+\tau) - \epsilon] - e^{-\zeta\omega(z+\tau)} \cos(\omega_d z - \epsilon) \right\}$$

$$g_r(z) = R_3\psi_3(z) + R_4\psi_4(z) = \frac{1}{2}\sqrt{2Bcsc}\frac{1}{2}\Theta\tau \sin[\Theta(z + \frac{1}{2}\tau) + \gamma] \quad (\text{B-1c})$$

$$g_q(z) = Q_3\psi_3(z) + Q_4\psi_4(z) = \frac{1}{2}\sqrt{2Bcsc}\frac{1}{2}\Theta\tau \cos[\Theta(z + \frac{1}{2}\tau) + \gamma] \quad (\text{B-1d})$$

where

$$R = \frac{\mu^2 R_0 B \sqrt{D^2 + F^2}}{\cosh \zeta \omega \tau - \cos \omega_d \tau} \quad \xi = \tan^{-1}(F/D)$$

$$Q = \frac{C \sqrt{E^2 + G^2}}{2(\cosh \zeta \omega \tau - \cos \omega_d \tau)} \quad \epsilon = \tan^{-1}(G/-E)$$

$$\gamma = \tan^{-1}(E/D).$$

Substituting from equation (B-1a) into equation (22c) and combining terms, we obtain

$$\hat{f}(\hat{t}) = R_0 \psi_0(\hat{t}) + \hat{C} \left\{ e^{-\zeta\omega \hat{t}} \cos[\omega_d(\hat{t} + \tau) - \phi] - e^{-\zeta\omega(\hat{t} + \tau)} \cos(\omega_d \hat{t} - \phi) \right\}, \quad (\text{B-2})$$

where

$$\hat{C} = \sqrt{R^2 + Q^2} e^{-2\zeta\omega(\tau - \frac{1}{c})} - 2(-1)^n R Q e^{-\zeta\omega(\tau - \frac{1}{c})} \cos(\xi - \epsilon + \omega\tau - \frac{\omega}{c})$$

$$\phi = \tan^{-1} \left[\frac{R \sin \xi - (-1)^n Q e^{-\zeta\omega(\tau - \frac{1}{c})} \sin(\epsilon + \frac{\omega}{c} - \omega\tau)}{R \cos \xi - (-1)^n Q e^{-\zeta\omega(\tau - \frac{1}{c})} \cos(\epsilon + \frac{\omega}{c} - \omega\tau)} \right]$$

Then,

$$\hat{f}(\hat{t}) = R_0 \psi_0(\hat{t}) + \hat{F} e^{-\zeta \omega \hat{t}} \cos(\omega_d \hat{t} - \phi - \psi), \quad (\text{B-3})$$

where

$$\hat{F} = \hat{C} \hat{D}, \quad D = \sqrt{(e^{-\zeta \omega \tau} - \cos \omega_d \tau)^2 + \sin^2 \omega_d \tau}, \quad (\text{B-4})$$

$$\psi = \tan^{-1} \left[\frac{\sin \omega_d \tau}{e^{-\zeta \omega \tau} - \cos \omega_d \tau} \right]. \quad (\text{B-5})$$

It follows from equation (22d) that

$$\begin{aligned} \hat{g}(\hat{t}) &= \frac{1}{2} \sqrt{2B} \csc \frac{1}{2} \Theta \tau \left\{ \sin \left[\Theta \left(\hat{t} + \frac{1}{2} \tau \right) + \gamma \right] - (-1)^n \cos \left[\Theta \left(\hat{t} + \frac{1}{2} \tau + \tau - \frac{1}{c} \right) + \gamma \right] \right\} \\ &= \frac{1}{2} \sqrt{2B} \csc \frac{1}{2} \Theta \tau \left(\hat{G} \sin \left[\Theta \left(\hat{t} + \frac{1}{2} \tau \right) + \gamma + \hat{\eta} \right] \right), \end{aligned}$$

where

$$\begin{aligned} \hat{G} &= \sqrt{\left[1 + (-1)^n \sin \Theta \left(\tau - \frac{1}{c} \right) \right]^2 + \left[\cos \Theta \left(\tau - \frac{1}{c} \right) \right]^2} \\ &= \sqrt{2 \{ 1 + (-1)^n [\sin \Theta \tau \cos \lambda - \cos \Theta \tau \sin \lambda] \}} \quad \left(\text{use } \cos \lambda_n \cong 0, \sin \lambda_n \cong (-1)^n \right) \\ &\cong 2 \sqrt{\frac{1}{2} (1 - \cos \Theta \tau)} = 2 \sin \frac{1}{2} \Theta \tau \\ \hat{\eta} &= \tan^{-1} \left[\frac{-(-1)^n \cos \Theta \left(\tau - \frac{1}{c} \right)}{1 - (-1)^n \sin \Theta \left(\tau - \frac{1}{c} \right)} \right] = \tan^{-1} \left[\frac{-\sin \Theta \tau}{1 + \cos \Theta \tau} \right]. \end{aligned}$$

Hence,

$$\hat{g}(\hat{t}) = \sqrt{2B} \sin \left[\Theta \left(\hat{t} + \frac{1}{2} \tau \right) + \gamma + \hat{\eta} \right]. \quad (\text{B-6})$$

APPENDIX C. FORMULATION OF EQUATION (40)

In the following, reformulate the typical terms contained in equation (40) into simple form:

1. The unit step functions

$$[u(t - k\tau) - u(t - k\tau - L/c)] = \begin{cases} 1 & k\tau \leq t \leq k\tau + L/c \\ 0 & k\tau + L/c \leq t \leq (k+1)\tau \end{cases}$$

$$\left[u(t - k\tau - 1/c) - u(t - k\tau - \frac{L+1}{c}) \right] = \begin{cases} 1 & k\tau + 1/c \leq t \leq k\tau + (L+1)/c \\ 0 & k\tau + (L+1)/c \leq t \leq (k+1)\tau + 1/c \end{cases}$$

2. The exponential functions

$$\sum_{k=0}^K \exp[-c\lambda(t - k\tau)] u(t - k\tau) - \exp[-c\lambda(t^* - k\tau - L/c)] u(t^* - k\tau - L/c)$$

$$= \begin{cases} - (e^{\lambda L} - 1) \frac{1 - e^{-c\lambda\tau(K+1)}}{1 - e^{-c\lambda\tau}} e^{-c\lambda t_0} & L/c \leq t_0 \leq \tau \\ - (e^{\lambda L} - 1) \frac{1 - e^{-c\lambda\tau K}}{1 - e^{-c\lambda\tau}} e^{-c\lambda(t_0 + \tau)} e + e^{-c\lambda t_0} & 0 \leq t_0 \leq L/c \end{cases}$$

where $t_0 = t - K\tau$ with $K\tau < t < (K+1)\tau$.

3. The sine functions

Making use of the identity,

$$\sum_{k=0}^K \sin k\theta = \sin \frac{1}{2}(K+1)\theta \sin \frac{1}{2}K\theta \csc \frac{1}{2}\theta,$$

we obtain

$$\sum_{k=0} \sin[\omega(t - k\tau) + \alpha] u(t - k\tau) - \sin[\omega(t - k\tau - L/c) + \alpha] u(t - k\tau - L/c)$$

$$\left\{ \begin{array}{l}
2\sin\frac{\omega L}{2c} \left\{ \sin\frac{1}{2}K\omega\tau \csc\frac{1}{2}\omega\tau \cos\left[\omega\left(t_0 + \frac{K-1}{2}\tau\right) + \phi\right] + \cos[\omega(t_0 + K\tau) + \phi] \right\} \\
\text{if } K\tau + L/c \leq t \leq (K+1)\tau \\
2\sin\frac{\omega L}{2c} \left\{ \sin\frac{1}{2}(K-1)\omega\tau \csc\frac{1}{2}\omega\tau \cos[\omega(t_0 + \frac{1}{2}K\tau) + \phi] + \cos[\omega(t_0 + K\tau) + \phi] \right\} \\
\text{if } K\tau \leq t \leq K\tau + L/c, \qquad \qquad \qquad + \sin(\omega t_0 + \alpha) ,
\end{array} \right.$$

where $\phi = \alpha - \omega L/2c$.

ON DYNAMIC RESPONSE OF A RECTANGULAR PLATE
TO A SERIES OF MOVING LOADS

By Frank C. Liu

The information in this report has been reviewed for security classification. Review of any information concerning Department of Defense or Atomic Energy Commission programs has been made by the MSFC Security Classification Officer. This report, in its entirety, has been determined to be unclassified.

This report has also been reviewed and approved for technical accuracy.



E. D. GEISLER

Director, Aero-Astroynamics Laboratory